Field-induced quantum criticality in low-dimensional Heisenberg spin systems

Mohamed Azzouz*
Department of Physics and Astronomy, Laurentian University, Ramsey Lake Road, Sudbury, Ontario, Canada P3E 2C6
(Received 24 May 2006; revised manuscript received 12 September 2006; published 20 November 2006)

We study the quantum critical behavior in the antiferromagnetic Heisenberg chain and two-leg Heisenberg ladder resulting from the application of an external magnetic field. In each of these systems a finite-temperature crossover line between two different ferromagnetic phases ends with a quantum critical point at zero temperature. Using the bond-mean-field theory, we calculate the field dependence of the magnetization and the mean-field spin bond parameters in both systems. For the Heisenberg chain, we recover the existing exact results and show in addition that the saturation of the zero-temperature magnetization at the field $h_c=2J$ is accompanied by a quantum phase transition, where the bond parameter vanishes. Here J is the exchange coupling constant along the chain. For the two-leg ladder, we also recover the known results, like the two magnetization plateaus, and show that at the upper critical field, which corresponds to the appearance of the saturation magnetization plateau, the chain and rung spin bond parameters vanish. The identification of the order parameters that govern the field-induced quantum criticality in the systems we study here constitutes an original contribution. Because no long-range order, which breaks symmetry, characterizes the bond order, the latter could be a proposal for the so-called hidden order. We calculate analytically the bond parameters in both systems as functions of the field in the low- and high-field limits at zero temperature. At nonzero temperatures, the calculation of the magnetization and bond parameters is carried out by solving the mean-field equations numerically.

DOI: 10.1103/PhysRevB.74.174422 PACS number(s): 75.10.Jm, 75.30.−m, 73.43.Nq

I. INTRODUCTION

According to Sachdev, a second-order quantum phase transition occurs in a system at absolute zero temperature when an order parameter vanishes at a critical value of a (an external) coupling parameter, like pressure or magnetic field.[1] Unlike classical phase transitions, which are driven by thermal fluctuations, a quantum phase transition is driven solely by quantum fluctuations. In this paper, we examine the occurrence of quantum criticality in two low-dimensional antiferromagnetic (AF) Heisenberg spin systems, which is induced by an external magnetic field. These systems are the Heisenberg chain and the two-leg Heisenberg ladder. To the best of our knowledge, quantum criticality was not addressed in these systems in the way we do here. We identify the microscopic parameters that govern the zero-temperature phase transition in these systems. These parameters are found to vary with, and vanish at, a critical value of the magnetic field.

Bonner and Fisher[2] and Parkinson and Bonner[3] have calculated the zero-temperature magnetization versus the magnetic field for the one-dimensional (1D) Heisenberg model and found that the magnetization reaches the saturation value M_s at the critical field $h_c=2J$ according to the law

$$\frac{M_z}{M_s}=1-\frac{4}{\pi}\left(1-\frac{h}{h_c}\right)^{1/2}, \tag{1}$$

which is valid for fields h slightly smaller than h_c. J is the spin exchange coupling constant. Note that for the Heisenberg chain the magnetization does not vanish abruptly at any value of the field; it increases linearly with the field near zero, then saturates at h_c. By analyzing the spin configuration, one finds that the latter evolves from the well-understood ground state with short-range AF order in zero field (a gapless spin liquid with algebraically decaying AF correlations and a correlation length $\xi=\infty$) to the ferromagnetic state with magnetization linearly increasing with field near zero, then finally to the fully saturated ferromagnetic ground state when $h>h_c$.[2,3] We find that the competition between the Ising and Zeeman interactions plays an important role in the way the magnetization depends on the field and that the unsaturated ferromagnetic state for $0<h<h_c$ is governed not only by the magnetization, but also by a parameter reflecting the AF Ising interaction and the quantum fluctuations: i.e., the spin bond parameter. This bond parameter decreases with increasing field, then vanishes at the critical value h_c, at which ferromagnetism reaches saturation. The unsaturated ferromagnetic state for $0<h<h_c$ can be called a quantum ferromagnet because quantum fluctuations prevent the saturation of the magnetic moment. For $h>h_c$ the ground state can be said to have classical ferromagnetism because the quantum fluctuations and Ising interaction are both irrelevant in this state. In sum, we show in this work that the saturation of the magnetization in the Heisenberg chain is accompanied by a second-order phase transition and identify and calculate the field dependence of the *order parameter* governing this phase transition.

The two-leg Heisenberg ladder is characterized by two bond parameters, one along the chains and the second one along the rungs. Also in this case, these bond parameters vanish when ferromagnetism reaches saturation at the upper critical field h_{c2}, which depends on the rung coupling. It is known that the two-leg Heisenberg ladder presents two magnetization plateaus: one zero-magnetization plateau for fields smaller than the lower critical field $h_{c1}=E_g$, where E_g is the energy gap, and the other plateau in the saturated ferromagnetic regime realized for fields greater than $h_{c2}>h_{c1}$.[4] Chitra and Giamarchi,[5] among many others, studied the two-leg ladder using the bosonization technique. They focused on the fields near h_{c1} and argued that a quantum critical transition occurs at this field. While we do not disagree with Chitra and

Giamarchi's treatment of the ladder, we will show that according to Sachdev's definition it is the point h_{c2} not h_{c1} that can be interpreted as a quantum critical point (QCP).

The justification for and importance of the present work stems from four reasons at least: first, from the importance of quantum criticality itself because 1D and two-leg ladder real systems exit. For example, the materials $Cu_2(C_5H_{12}N_2)_2Cl_4$ and $(C_5H_{12}N_2)_2CuBr_4$ are two-leg Heisenberg ladders for which the results and predictions of this paper can be applied because the magnetic fields needed to attain magnetization saturation can be realized in laboratories due to the weakness of the exchange coupling constants in these systems.[4,6] In fact, the phase diagram we calculate for the ladder agrees well with the phase diagram Chaboussant *et al.*[7] proposed for the material $Cu_2(C_5H_{12}N_2)_2Cl_4$ using the nuclear magnetic resonance experimental technique. Second, the results we get here may contribute to the understanding of quantum criticality in other real systems like high-T_C materials. For both systems we consider here, we find that a finite-temperature crossover line ends with a QCP at zero temperature. For high-temperature superconductors, the proposed QCP in the doping-temperature phase diagram is of this kind; i.e., it is believed that the pseudogap appears below a crossover doping-dependent temperature that defines a line that ends with a QCP near optimal doping.[8] Third, the quantum critical points we examine take place within a magnetically ordered state; the quantum phase transitions here are not from a disordered state to an ordered one. Likewise, the proposed QCP in high-temperature superconductors takes place within the superconducting state, which is also an ordered state. The fourth reason is that, as we already mentioned earlier, we identify the microscopic parameter that gives rise to the QCP.

This paper is organized as follows. In Sec. II, we explain the mean-field theory used to study the quantum phase transition in the 1D Heisenberg model. In Sec. III, we calculate the field dependence of the bond parameter for the Heisenberg chain and show that a phase transition takes place at zero temperature, but no nonzero-temperature phase transition occurs. In Sec. IV, we calculate the spin bond-bond correlation function and show that it undergoes a drastic change at the critical field of the transition. In Sec. V, we study quantum criticality and analyze the field dependence of the uniform spin susceptibility in the two-leg ladder. In Sec. VI, we summarize the results of this work using the field-temperature phase diagrams. In Sec. VII, we present the conclusions of this work.

II. QUANTUM PHASE TRANSITION IN THE HEISENBERG CHAIN

A. Approach description

We begin by explaining the improvements we made in this work to the zero-field bond-mean-field theory[9] (BMFT) for the Heisenberg chain. Then, we extend the BMFT to the case when an external magnetic field is applied to the chain.

1. Zero-field BMFT

The 1D Heisenberg model is

$$H_{1D} = J\sum_{\langle i,j\rangle} \mathbf{S}_i \cdot \mathbf{S}_j, \tag{2}$$

where $\mathbf{S}_i$ is the spin-1/2 operator at site i and $\langle i,j\rangle$ designates the sum over adjacent sites only. Using the well-known 1D Jordan-Wigner (JW) transformation

$$S_i^- = c_i e^{i\phi_i}, \quad \phi_i = \sum_{j=0}^{i-1} n_i,$$

$$S_i^z = n_i - 1/2, \tag{3}$$

with $n_i = c_i^\dagger c_i$, the Heisenberg chain maps onto a Hamiltonian of 1D interacting spinless fermions; i.e.,

$$H_{1D} = \frac{J}{2}\sum_i (c_i^\dagger c_{i+1} + \text{H.c.}) + J\sum_i \left(c_i^\dagger c_i - \frac{1}{2}\right)\left(c_{i+1}^\dagger c_{i+1} - \frac{1}{2}\right). \tag{4}$$

In the framework of the BMFT, we consider the bond parameter $\langle c_i c_{i+1}^\dagger\rangle$ to decouple the Ising quartic term in Eq. (4). The procedure is as follows. By neglecting the fluctuations in $\langle c_i c_{i+1}^\dagger\rangle$, we write

$$\begin{aligned} c_i^\dagger c_i c_{i+1}^\dagger c_{i+1} &\approx \langle c_i c_{i+1}^\dagger\rangle c_i^\dagger c_{i+1} + \langle c_{i+1} c_i^\dagger\rangle c_{i+1}^\dagger c_i + \langle c_i c_{i+1}^\dagger\rangle\langle c_{i+1} c_i^\dagger\rangle \\ &= Q_i c_i^\dagger c_{i+1} + Q_i^* c_{i+1}^\dagger c_i + |Q_i|^2, \end{aligned} \tag{5}$$

with $Q_i = \langle c_i c_{i+1}^\dagger\rangle$ the mean-field bond parameter. Note that $|\langle S_i^- S_{i+1}^+\rangle| = |\langle c_i c_{i+1}^\dagger\rangle|$, which means that the parameter Q_i accounts for the quantum fluctuations in the Heisenberg Hamiltonian. To recover a result comparable to the des Cloiseaux–Pearson[10] spin-excitation spectrum for the single Heisenberg chain, namely,

$$E(k) = J\frac{\pi}{2}|\sin k|, \tag{6}$$

one has to choose $Q_i = (-1)^i Q \equiv Q e^{i\pi x_i}$, where Q is site independent. Here, x_i is an integer that labels the site coordinate along the Heisenberg chain. This yields a phase configuration along the chain of the form $\pi x_i \equiv \ldots, \pi, 0, \pi, 0, \ldots$, which will in turn give[9]

$$E(k) = J_1|\sin k|, \tag{7}$$

when the single-fermion term (the XY term) is also written within the alteranted phase scheme. The hopping amplitude for the JW fermions resulting from this treatment is $(-1)^i J_1$, with $J_1 = J(1+2Q)$ indicating that a renormalization of the single-particle term in Eq. (4) by the Ising interaction took place. Choosing a uniform Q_i and neglecting the alternation of the sign of XY-hopping amplitude gives a $\cos k$ spectrum that does not agree with the des Cloiseaux–Pearson result.

Physically, we can justify the choice of the staggered Q_i in the following way. Consider two adjacent bonds $(2i, 2i+1)(2i+1, 2i+2)$. Because of the AF correlations, the bonds $(2i, 2i+1)(2i+1, 2i+2)$ may be in the spin configuration $(\uparrow_{2i}, \downarrow_{2i+1})(\downarrow_{2i+1}, \uparrow_{2i+2})$. Using the argument of only short-range and short-lived AF order, one has to view the object $(\uparrow_{2i}, \downarrow_{2i+1})$ as a renormalized spin singlet, rather than a static spin arrangement, because of the important spin fluctuations.

In the mean-field treatment based on the JW fermions, any two adjacent bonds can be quantitatively represented by the product $\langle c_{2i}^{\dagger}c_{2i+1}\rangle\langle c_{2i+1}c_{2i+2}^{\dagger}\rangle$, which turns out to be $-Q^2$, since $Q=\langle c_{2i+1}c_{2i+2}^{\dagger}\rangle$ and $\langle c_{2i}^{\dagger}c_{2i+1}\rangle=-\langle c_{2i+1}c_{2i}^{\dagger}\rangle=-Q$. It is thus justified to use opposite signs for Q on adjacent bonds. We assumed that creating a JW fermion is equivalent to having a spin-up state and destroying a JW fermion corresponds to a spin-down state.

With all this and Eq. (5), the mean-field Hamiltonian takes on the form

$$H_{1D}=NJQ^2+\sum_k \Psi_k^{\dagger}\mathcal{H}_{1D}\Psi_k, \tag{8}$$

where the spinor Ψ is given by

$$\Psi_k^{\dagger}=(c_k^{A\dagger}c_k^{B\dagger}) \tag{9}$$

and the Hamiltonian density by

$$\mathcal{H}=\begin{pmatrix}0 & e(k)\\ e^*(k) & 0\end{pmatrix}, \tag{10}$$

with $e(k)=iJ_1\sin k$. c_k^{η} is the Fourier transform of c_i^{η}. $\eta=A$ or B is the label of the two AF sublattices. The eigenenergies are $E_{\pm}(k)=\pm J(1+2Q)|\sin k|$. The ground-state energy per site is

$$E_{GS}=JQ^2-\frac{1}{2\beta}\int\frac{dk}{2\pi}\sum_{p=\pm}\ln[1+e^{-\beta E_p(\mathbf{k})}], \tag{11}$$

which gives $E_{GS}(T=0)=JQ^2-\frac{1}{\pi}J(1+2Q)$ at zero temperature because only the band with negative energies is filled at this temperature. Minimizing E_{GS} with respect to Q gives $Q=1/\pi$ at $T=0$. At nonzero temperature Q is given by

$$Q=-\frac{1}{2}\int\frac{dk}{2\pi}|\sin k|\sum_{p=\pm}pn_F[E_p(k)]. \tag{12}$$

Here, $n_F[E_p(k)]=1/[1+e^{\beta E_p(k)}]$ is the Fermi-Dirac factor. In the high-T limit with $k_BT\gg J$, we get $Q\approx\frac{J}{8k_BT}\frac{1}{1-4k_BT/J}$, a result that rules out any finite-T phase transition, in agreement with the Mermin-Wagner theorem.[11] Next, we will extend the analysis we just finished to the case of a Heisenberg chain coupled to an external magnetic field.

2. Nonzero-field BMFT

Existing numerical data prove that the magnetization becomes nonzero as soon as a magnetic field is applied to the Heisenberg chain. This suggests that the parameter $\langle S_i^z\rangle$ has to be included in the decoupling procedure of the Ising term when the magnetic field is oriented along the z axis. Hence we write

$$\begin{aligned}JS_i^zS_{i+1}^z&\approx J\langle S_i^z\rangle S_{i+1}^z+J\langle S_{i+1}^z\rangle S_i^z-J\langle S_i^z\rangle\langle S_{i+1}^z\rangle\\&\approx JM_zc_{i+1}^{\dagger}c_{i+1}+JM_zc_i^{\dagger}c_i-JM_z^2-JM_z,\end{aligned} \tag{13}$$

with $M_z=\langle S_i^z\rangle$ being the magnetization per site. In the presence of the Zeeman coupling term $g\mu_BB\Sigma_iS_i^z$, the mean-field Hamiltonian becomes

$$H_{1D}(h)=NJQ^2+Nh/2-NM_z(M_z+1)J+\sum_k\Psi_k^{\dagger}\mathcal{H}_{1D}(h)\Psi_k. \tag{14}$$

Now, the Hamiltonian density is given by

$$\mathcal{H}_{1D}(h)=\begin{pmatrix}2M_zJ-h & e(k)\\ e^*(k) & 2M_zJ-h\end{pmatrix}, \tag{15}$$

where $h=g\mu_BB$, B being the magnetic field, g the Landé factor, and μ_B the Bohr magneton. Interestingly, contrary to the current belief, we find that the magnetic field alone is not the chemical potential for the JW fermions. Rather, the chemical potential is given by $h-2M_zJ=h(1-2J\chi)$ if $h\ll J$ or by $h-J$ if $h>h_c$. χ is the uniform spin susceptibility. Diagonalizing Eq. (15) yields the following energy eigenvalues:

$$E_{\pm}(k)=2M_zJ-h\pm|e(k)|.$$

The free energy per site is

$$f=\frac{h}{2}-M_z(M_z+1)J+JQ^2-\frac{1}{2\beta}\int\frac{dk}{2\pi}\sum_{p=\pm}\ln[1+e^{-\beta E_p(\mathbf{k})}]. \tag{16}$$

Calculating the magnetization per site, $M_z=-\partial f/\partial h$, and minimizing f with respect to Q yields

$$\begin{aligned}Q&=-\frac{1}{2}\int\frac{dk}{2\pi}|\sin k|\sum_{p=\pm}pn_F[E_p(k)],\\M_z&=\frac{1}{2}\int\frac{dk}{2\pi}\sum_{p=\pm}n_F[E_p(k)]-\frac{1}{2},\end{aligned} \tag{17}$$

where now Q depends on field h. Because E_p depends on M_z, the equation determining M_z is self-consistent.

The analysis of the mean-field equations (17) reveals the existence of a zero-T phase transition at the field $h_c=2J$ where the parameter Q vanishes. This is what we report on in the next section.

III. FIELD-DRIVEN QUANTUM PHASE TRANSITION IN THE CHAIN

A. Numerical solution

For a strong field ($h>h_c$ as it turns out), the Fermi-Dirac factors in the expression for M_z in Eqs. (17) become all equal to 1 at zero temperature. This leads to $M_z=1/2$ in this limit. Also, Q vanishes when the field satisfies $2M_zJ-h+E_+(k)<0$ for any wave number k, because the difference of the Fermi-Dirac factors in the equation for Q in (17) is zero in this limit. Letting $M_z=1/2$ when the field is large and letting $k=\pi/2$, which gives the highest energy, yields $h>h_c$, with $h_c=2J$ for the critical field.

In order to understand how this critical field comes into play, we plot the excitation energy $E_+(k)$ as a function of the wave number k for three values of the field in Fig. 1. In zero field, the chemical potential of the JW fermions is zero, so

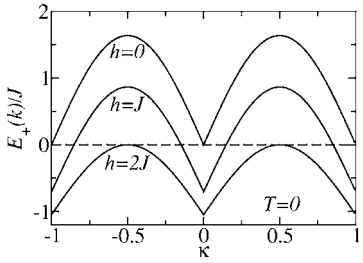

FIG. 1. The energy spectrum $E_+(k)$ of the 1D Heisenberg model is displayed as a function of $\kappa=k/\pi$ for three magnetic field values. The dashed line represents the chemical potential of the JW fermions in zero field. The bandwidth decreases with increasing field h when $h<h_c$.

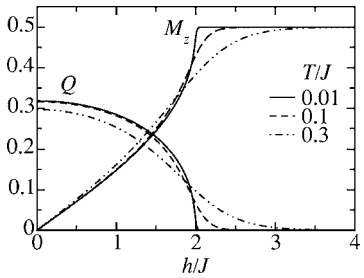

FIG. 2. The parameter Q and the magnetization M_z are plotted as functions of h for three values of temperature. At $T=0$, Q vanishes at $h_c=2J$, where M_z reaches its saturation value (see text). At finite temperature, the singularity in the first derivative of M_z with respect to h is replaced by a smooth crossover as seen for all three temperatures here.

only the lower-energy band with energy $E_-(k)$ is filled. As the field is increased, the chemical potential for the JW fermions increases, leading to an increase in the population of the higher-energy band $E_+(k)$. For example, for $h=J$ only part of this band is filled, but for $h>2J$ the whole higher-energy band is filled as is illustrated in Fig. 1. Increasing further the field above $2J$ does not affect the population of the higher-energy band any more. This results in the saturation of the magnetization M_z because M_z is related to the total number of the JW fermions as the second of Eqs. (17) shows.

Figure 2 shows the parameter Q and the magnetization M_z as functions of the field h. The field dependence shown here by M_z is in very good agreement with the result of Ref. 3 obtained using the Lanczös method. Clearly, one can see that Q vanishes at $h\simeq h_c=2J$ for the lowest temperature $T=0.01J$. We will show in Sec. III B 2 that at zero temperature Q vanishes at h_c with the power exponent 1/2. This behavior signals the occurrence of a phase transition, which is governed by the bond parameter Q. We label the state with $Q>0$ for $h<h_c$ as being characterized by bond order because Q is a spin bond parameter. Interestingly, the bond order competes with ferromagnetic order, and when the latter reaches its saturation level at h_c, the bond order disappears altogether. For $0<h<h_c$, the state is characterized by both bond order and unsaturated ferromagnetism; for this reason, this state is called a quantum ferromagnet. When temperature is nonzero (see the curves for $T=0.01J$, $0.1J$, and $0.3J$ in Fig. 2) the singularity in $\chi=\partial M_z/\partial h$ is replaced by a nonsingular behavior, and Q goes to zero rather smoothly when field increases. The critical behavior occurs at $T=0$ only.

It is possible to calculate analytically approximate zero-temperature solutions for the mean-field equations in the strong- and weak-field limits. We will next show the results of such a calculation.

B. Analytical zero-temperature solution

1. Behavior in the low-field regime

In this section, we calculate analytically the zero-T field dependence of Q in the low-field limit. At very low temperatures, only low-energy excitations contribute to the Fermi-Dirac factors. In these limits, we obtain an approximate expression for Q by replacing $|\sin k|$ in $E_p(k)$ by $|k|$ in the Fermi-Dirac factors. For $\beta=\infty$, $n_F(E_-)-n_F(E_+)=1$ for $(h-2M_zJ)/J_1<k<\pi/2$. Using Eqs. (17), one gets

$$Q\approx\frac{1}{\pi}\cos\left(\frac{h-2M_zJ}{J_1}\right)\approx\frac{1}{\pi}-\frac{1}{2\pi}\frac{(1-2J\chi)^2}{(1+2/\pi)^2}\left(\frac{h}{J}\right)^2,\quad h\ll J, \tag{18}$$

where we replaced J_1 by its zero-field and zero-temperature value; $J_1=J(1+2/\pi)$ because $Q=1/\pi$ in this case, and the magnetization is given by $M_z=\chi h$ when $h\ll J$. Equation (18) shows that Q decreases quadratically when field increases in the vicinity of zero.

To calculate the susceptibility χ in the vicinity of zero field, we expand the Fermi-Dirac factors in the expression of M_z in Eqs. (17) and use $M_z\approx\chi h$. To first order, one gets

$$M_z=\frac{1}{2}\int\frac{dk}{2\pi}\sum_{p=\pm}n_F[E_p(k,h=0)]-\frac{1}{2}+\frac{2M_zJ-h}{2}\int\frac{dk}{2\pi}\sum_{p=\pm}\left.\frac{\partial n_F}{\partial E_p}\right|_{h=0}. \tag{19}$$

Using the fact that in the absence of a magnetic field the magnetization is zero, i.e., only the lower-energy band is filled with JW fermions at zero temperature,

$$\frac{1}{2}\int\frac{dk}{2\pi}\sum_{p=\pm}n_F[E_p(k,h=0)]=\frac{1}{2},$$

one finds the uniform magnetic susceptibility χ (for the response along the z axis) to be

$$\chi=\frac{\chi_0}{1+2J\chi_0}, \tag{20}$$

where

$$\chi_0=-\frac{1}{2}\int\frac{dk}{2\pi}\sum_p\left.\frac{\partial n_F}{\partial E_p}\right|_{h=0}$$

is the susceptibility in the absence of the self-consistent term $2JM_z$ in $E_p(k)$. At zero temperature ($\beta=\infty$),

$$\chi_0 = \frac{1}{2}\int \frac{dk}{2\pi}\sum_p \delta[E_p(h=0)] = \frac{1}{\pi v_s}, \tag{21}$$

with $v_s = J(1+2Q)$. We emphasize that Eq. (20) is valid in the linear-response regime when $h \ll J$. Also, Eq. (20) shows that the susceptibility in the present treatment consists of an infinite series of the powers of the susceptibility χ_0; i.e., it is of the random-phase-approximation (RPA) form. This is a significant improvement from the case where only χ_0 was considered.[12,13] Note that $J\chi_0 \sim 0.2$ near zero temperature, so that using $\chi \approx \chi_0$ remains only qualitatively acceptable in the linear-response regime ($h \ll J$) at low temperatures. Equation (20) shows that the Ising interaction reduces the uniform susceptibility because of the tendency of the Ising term to form AF ordering; the term $2J\chi_0$ in the denominator results from the Ising interaction. Figure 3 displays both χ and χ_0 as functions of temperature in zero magnetic field. Note that $J\chi \approx 0.14$ at zero temperature yields $J\chi_0 \approx 0.194$ in agreement with Eq. (21). Clearly, χ deviates significantly from χ_0 at low temperature. The fact that χ is smaller than χ_0 at low temperature is an indication that quantum fluctuations are treated better in the present RPA-type approximation.

2. Behavior near the critical region

At zero temperature, both Fermi-Dirac factors at $E_{\pm}(k)$ become equal to 1 when the field is greater than $h_c = 2J$. Q vanishes and $M_z = 1/2$ for $h > h_c$. For h slightly below h_c, Q and M_z are found to behave as

$$Q = \frac{2}{\pi}\left(1 - \frac{h}{h_c}\right)^{1/2},$$

$$\frac{M_z}{M_s} = 1 - \frac{4}{\pi}\left(1 - \frac{h}{h_c}\right)^{1/2}, \tag{22}$$

where $M_s = 1/2$ is the saturation value for the magnetization. The equation for M_z near criticality is the same as that of Parkinson and Bonner (see Ref. 3 and references therein). In this regime, the susceptibility diverges at h_c^- with the critical exponent 1/2:

$$\chi = \frac{2}{\pi h_c}\left(1 - \frac{h}{h_c}\right)^{-1/2} \quad (h \sim h_c). \tag{23}$$

We now explain how we obtained the equation for Q. In Eqs. (17), we again replace $\sin k$ in the Fermi-Dirac factors by k and get for Q

$$Q = \frac{1}{\pi}\int_{k_0}^{\pi/2} dk \sin k = \frac{1}{\pi}\left[1 - \left(\frac{h-J}{J_1}\right)^2\right]^{1/2}, \tag{24}$$

with $k_0 = \arcsin[(h-J)/(J_1)]$. For h near h_c, we let $Q=0$ in J_1 and define $\delta = h_c - h$ where δ is very small. This yields

$$Q \approx \frac{\sqrt{2}}{\pi}\sqrt{\delta/J}, \tag{25}$$

which in turn gives the result in Eqs. (22). Equation (25) is found to agree with the numerical result for Q displayed in Fig. 2.

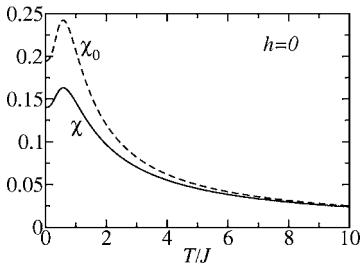

FIG. 3. The self-consistent magnetic susceptibility χ and the susceptibility χ_0 are plotted as functions of temperature for zero field. Clearly, χ and χ_0 differ significantly at low temperature, but are practically equal at very high temperature.

The vanishing of Q at h_c indicates that a zero-temperature phase transition takes place at h_c. This transition is accompanied by the saturation of the magnetization M_z. It is noteworthy that this phase transition occurs at the minimum magnetic field required to suppress the contribution from the bond order to the total free energy. Remember that Q is given rise to by the decoupling of the Ising term in the Heisenberg model. When this happens—i.e., for $h > h_c$—the contribution to free energy comes only from the XY and Zeeman terms and also from the decoupling of the Ising term in the Zeeman canal (M_z terms).

To interpret this transition, which takes place at zero temperature, as a quantum phase transition, we need examine the second ingredient necessary for a quantum phase transition: namely, a drastic change in the correlations attributed to the "order" parameter that vanishes at the critical field h_c.[1] We will next show that the Ising term is responsible for bond-bond order below the critical field h_c. Above h_c, this bond-bond order disappears.

IV. BOND-BOND CORRELATION FUNCTION

In the presence of any nonzero magnetic field, the magnetization becomes finite, hence leading to the breakdown of the SU(2) symmetry. However, the quantum phase transition is not governed by the magnetization along the z axis, but rather by the spin-bond correlations in the xy plane of the spin degrees of freedom. We consider the correlations between two bonds (AB) at (the Matsubara) time $\tau = 0$ and (BA) at time τ, and a distance R apart from each other. We calculate the bond-bond correlation function defined in the following way:

$$\begin{aligned}
&\langle T_\tau S_0^{A+}(0) S_1^{B-}(0) S_R^{B-}(\tau) S_{R+1}^{A+}(\tau)\rangle \\
&\quad \propto -\langle T_\tau c_0^{A\dagger}(0) c_1^B(0) c_R^B(\tau) c_{R+1}^{A\dagger}(\tau)\rangle \\
&\quad = -\langle c_0^{A\dagger}(0) c_1^B(0)\rangle\langle c_R^B(\tau) c_{R+1}^{A\dagger}(\tau)\rangle \\
&\qquad -\langle T_\tau c_R^B(\tau) c_0^{A\dagger}(0)\rangle\langle T_\tau c_1^B(0) c_{R+1}^{A\dagger}(\tau)\rangle \\
&\quad = -Q^2 - G^{BA}(R,\tau) G^{BA}(-R,-\tau) \\
&\quad = -Q^2 + \frac{1}{\beta}\sum_m \int \frac{dq}{2\pi}\chi_b(q, i\omega_m) e^{i(Rq+\tau\omega_m)},
\end{aligned} \tag{26}$$

where we have used for the equal-time averages $\langle c_1^B(0)c_0^{A\dagger}(0)\rangle=-Q$ on bond AB between sites 0 and 1 and $\langle c_R^B(\tau)c_{R+1}^{A\dagger}(\tau)\rangle=Q$ for bond BA between sites R and $R+1$. Note that $R=1$ corresponds to the nearest-neighbor bond correlations. The first line in Eq. (26) is obtained using the JW transformation and the second one using Wick's theorem for fermions.

The Green's function is defined by

$$G^{BA}(R,\tau)=-\langle T_\tau c_R^B(\tau)c_0^{A\dagger}(0)\rangle \tag{27}$$

and the bond response function by

$$\chi_b(q,i\omega_m)=-\frac{1}{\beta}\sum_n\int\frac{dk}{2\pi}G^{BA}(k,i\omega_n)G^{BA}(k+q,i\omega_n+i\omega_m), \tag{28}$$

where $i\omega_n$ and $i\omega_m$ are the fermion and boson Matsubara frequencies, respectively. The subscript b in χ_b refers to bond. The matrix of the Green's functions is

$$\mathcal{G}=(i\omega_n-\mathcal{H}_{1D})^{-1}=\begin{pmatrix}G^{AA} & G^{AB}\\ G^{BA} & G^{BB}\end{pmatrix}, \tag{29}$$

with

$$G^{AA}=G^{BB}=\frac{1}{2}\left(\frac{1}{i\omega_n+h'-|e|}+\frac{1}{i\omega_n+h'+|e|}\right),$$

$$G^{AB}=\frac{1}{2}e^{i\phi}\left(\frac{1}{i\omega_n+h'-|e|}-\frac{1}{i\omega_n+h'+|e|}\right),$$

$$G^{BA}=\frac{1}{2}e^{-i\phi}\left(\frac{1}{i\omega_n+h'-|e|}-\frac{1}{i\omega_n+h'+|e|}\right). \tag{30}$$

Here $e^{i\phi(k)}=e(k)/|e(k)|$. Performing the summation over the Matsubara frequencies yields

$$\chi_b(q,i\omega_m)=-\frac{1}{4}\int\frac{dk}{2\pi}e^{-i[\phi(k)+\phi(k+q)]}\sum_{p=0}^{1}\sum_{p'=0}^{1}(-1)^{p+p'}\frac{n_F[(-1)^p|e(k)|-h']-n_F[(-1)^{p'}|e(k+q)|-h']}{(-1)^p|e(k)|-(-1)^{p'}|e(k+q)|+i\omega_m}, \tag{31}$$

with $h'=h-2M_zJ$. It is interesting to note that in the strong-field limit ($h>h_c=2J$), both the lower- and higher-energy bands are fully occupied even at zero temperature. This implies that the Fermi-Dirac factors in Eq. (31) are both equal to 1 in this limit, a result that leads to $\chi_b=0$. Also, we have seen that $Q=0$ when $h>h_c$, which means that the bond-bond correlations vanish altogether in this case. In the limit of a weak field, however, the term Q^2, which is nonzero, dominates in (26) when the distance R is large. The term in χ_b yields small corrections that decay with distance R. This shows that at $h_c=2J$ the bond-bond correlations undergo a drastic change. Thus, all the ingredients necessary for the field-driven quantum phase transition in the Heisenberg chain are satisfied: namely, that an order parameter vanishes under the effect of a coupling (here the magnetic field) and the occurrence of a drastic change in the correlation function associated with this order parameter.

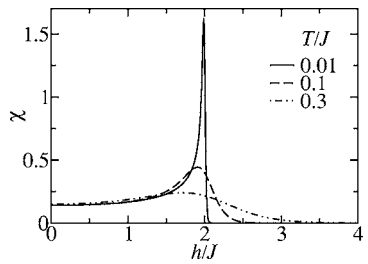

FIG. 4. The uniform spin susceptibility $\chi(h)=\partial M_z/\partial h$ is plotted versus field h for three different temperatures. Note that $\chi_b(0,0)\sim\chi$.

To illustrate the sudden change of behavior at h_c, we calculate the uniform and static bond susceptibility χ_b, which we find to be given by

$$\chi_b(0,0)\sim\chi, \tag{32}$$

where χ is the uniform field-dependent spin susceptibility. Figure 4 shows χ as a function of h for three different temperatures. Very close to zero temperature, for $T=0.01J$ in Fig. 4, χ displays a sharp asymmetric peak at h_c. This peak broadens when temperature increases. We showed earlier [see Eq. (23)] that at zero temperature, χ is singular at h_c with the exponent of the singularity for $h<h_c$ being 1/2. χ drops sharply at h_c^+, but becomes nonzero as temperature increases because the singularity in the derivative of M_z at h_c disappears as soon as T becomes finite. Note that, in addition to this sharp change in $\chi_b(0,0)$ at h_c, the term in Q^2 in (26) also undergoes a sharp, but not diverging, change at h_c.

V. QUANTUM CRITICALITY IN THE TWO-LEG LADDER

A. Derivation of the mean-field equations

In this section, we will study the quantum criticality arising from an external magnetic field in the two-leg Heisenberg ladder. The Hamiltonian for such a system is

$$H_{2L} = J\sum_i \sum_{j=1}^{2} \mathbf{S}_{i,j}\cdot\mathbf{S}_{i+1,j} + J_\perp \sum_i \mathbf{S}_{i,1}\cdot\mathbf{S}_{i,2} - h\sum_i \sum_{j=1}^{2} S^z_{i,j}, \tag{33}$$

where $J_\perp$ is the exchange coupling along the rungs, J the coupling along the chains, and $i=1,\ldots,N$ and $j=1,2$ are the site index along the chains and the chain label, respectively. N is the number of sites on each of the chains, giving the total number of sites of the ladder to be $2N$. Here, we extend to the case of a ladder in a finite magnetic field the approach developed for the two-leg ladder in zero field in Ref. 14. Performing the Fourier transform along the chains while keeping the chain labels in the real space gives the following mean-field Hamiltonian:

$$H_{2L} = -N(2J+J_\perp)M_z(M_z+1) + Nh + 2NJQ^2 + NJ_\perp P^2 + \sum_k \Psi_k^\dagger \mathcal{H}_{2L}\Psi_k, \tag{34}$$

where

$$\Psi_k^\dagger = (c_{1k}^{A\dagger} c_{1k}^{B\dagger} c_{2k}^{A\dagger} c_{2k}^{B\dagger}) \tag{35}$$

and

$$\mathcal{H}_{2L} = \begin{pmatrix} -h' & e(k) & 0 & \frac{J_{\perp 1}}{2} \\ e^*(k) & -h' & \frac{J_{\perp 1}}{2} & 0 \\ 0 & \frac{J_{\perp 1}}{2} & -h' & e(k) \\ \frac{J_{\perp 1}}{2} & 0 & e^*(k) & -h' \end{pmatrix} \tag{36}$$

is the Hamiltonian density. Here, $h'=h-(2J+J_\perp)M_z$, $e(k)=iJ_1\sin k$, with $J_1=J(1+2Q)$ and $J_{\perp 1}=J_\perp(1+2P)$. The parameter Q is defined in the same way along the chains as for the single Heisenberg chain, but $P=\langle c_{i,1}c_{i,2}^\dagger\rangle$ is the bond parameter along the rungs of the ladder. Physically, P has the same meaning as Q; i.e., P accounts for the strength of the rung singlets because $P=\langle c_{i,1}c_{i,2}^\dagger\rangle \equiv |\langle S_{i,1}^- S_{i,2}^+\rangle|$. One can think of Q and P as being two values for the same physical parameter that is spatially anisotropic as a result of J and $J_\perp$ being generally different, and because of the ladder geometry. The mean-field energy spectra, which are given by

$$E_\pm(k) = -h' \pm \sqrt{J_1^2\sin^2 k + J_{\perp 1}^2/4}, \tag{37}$$

depend only on the longitudinal wave vector k. Note that because we did not perform a Fourier transform perpendicular to the chains, there is no $k_\perp$ dependence in $E_\pm$ (k). As Eq. (35) shows, the chain index (1 or 2) appears in the spinor ψ_k in stead of $k_\perp$. $E_\pm(k)$ are characterized by the energy gap $E_g=J_{\perp 1}/2$ at $k=0$ or π. Obviously, this is not completely accurate because exact numerical methods have indicated that the gap at $k=0$ is greater than the gap at $k=\pi$.[16,17] The energy gap we find here is between the exact gaps at $k=0$ and $k=\pi$; one can thus think of the gap we find as a mean-field average of the true gaps. Note that for the purpose of studying the quantum phase transition in the two-leg ladder, the shape of the spectrum is not as crucial as the presence of the energy gap itself. We will indeed see that our results are qualitatively correct since they compare well with existing exact numerical data for the magnetization versus field. Among the first researchers to have studied the two-leg ladder system we find Dagotto *et al.*,[15] Barnes *et al.*,[16] and Barnes and Riera.[17] More recently, Dai and Su[18] have proposed a different theory, also based on the JW transformation, that gave an energy spectrum with the correct behavior near 0 and π. Their theory, as they have found, is, however, not valid in the limit $\alpha\to 0$ for the energy gap because the gap does not vanish with α. Therefore, we would rather use the BMFT, which is valid in this limit. Here, $\alpha=J_\perp/J$.

The mean-field free energy per site is

$$f_{2L}(T,h) = JQ^2 + \frac{1}{2}J_\perp P^2 - \frac{1}{2}(2J+J_\perp)M_z(M_z+1) + \frac{h}{2} - \frac{1}{2\beta}\int \frac{dk}{2\pi}\sum_{p=\pm} \ln[1+e^{-\beta E_p(k)}]. \tag{38}$$

Minimizing the free energy with respect to Q and P and calculating the magnetization yields the following mean-field equations:

$$Q = \frac{1}{2}\int \frac{dk}{2\pi}\frac{J_1\sin^2 k_x}{\epsilon(k)}\{n_F[E_-(k)] - n_F[E_+(k)]\},$$

$$P = \frac{1}{4}\int \frac{dk}{2\pi}\frac{J_{\perp 1}}{\epsilon(k)}\{n_F[E_-(k)] - n_F[E_+(k)]\},$$

$$M_z = \frac{1}{2}\int \frac{dk}{2\pi}\sum_{p=\pm} n_F[E_p(k)] - \frac{1}{2}, \tag{39}$$

with

$$\epsilon(k) = \sqrt{J_1^2\sin^2 k + J_{\perp 1}^2/4}. \tag{40}$$

We will next analyze analytically these mean-field equations in several limiting cases: like in zero field and temperature, in zero field and high temperature, in zero temperature and weak field, and in zero temperature and in the vicinity of the critical field.

B. Analytical analysis of the mean-field equations

1. Zero-field and zero-temperature regime

We start by examining the zero-field and zero-temperature solution. In fact we report here new analytical results in this limit, which were not published in Ref. 14. Using the elliptic functions E and F in the small-α limit, we obtain

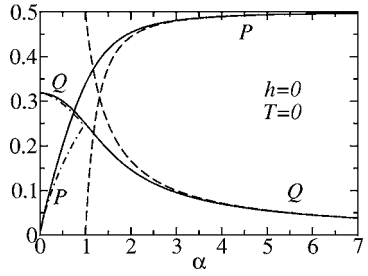

FIG. 5. Q and P are plotted as functions of α. The solid lines represent the numerical calculation results. The dash-dotted and dashed lines are the approximate analytical results of Eqs. (42) for small α and Eqs. (44) for large α.

$$Q \approx \frac{1}{\pi} E\left(\frac{\pi}{2}, y\right) - \frac{J_{\perp 1}^2}{4\pi J_1^2} F\left(\frac{\pi}{2}, y\right),$$

$$P \approx \frac{J_{\perp 1}}{2\pi J_1} F\left(\frac{\pi}{2}, y\right), \tag{41}$$

with $y = 2J_1/\sqrt{J_{\perp 1}^2 + 4J_1^2}$. Expanding the functions E and F when α is small ($\alpha \ll 1$) leads to

$$Q \approx \frac{1}{\pi} - \frac{\alpha^2}{4\pi(1+2/\pi)^2} \ln\left(\frac{8(1+2/\pi)}{\alpha}\right),$$

$$P \approx \frac{\alpha}{2\pi(1+2/\pi)} \ln\left(\frac{8(1+2/\pi)}{\alpha}\right) \quad (\alpha \ll 1). \tag{42}$$

The energy gap in this limit is given by

$$E_g \approx \frac{J_\perp}{2}\left\{1 + \frac{\alpha}{\pi(1+2/\pi)} \ln\left[\frac{8(1+2/\pi)}{\alpha}\right]\right\}. \tag{43}$$

Note that $P \sim \alpha \ln \alpha$ when α is very small and that the contribution to Q from the transverse coupling behaves as $\alpha^2 \ln \alpha$.

In the large-coupling limit with $\alpha \gg 1$ along the ladder rungs, Q and P are approximately given by

$$Q \approx \frac{1}{4\alpha - 2},$$

$$P \approx \frac{1}{2}\left[1 - \left(\frac{1}{2\alpha - 1}\right)^2\right] \quad (\alpha \gg 1), \tag{44}$$

which means that $Q \sim 1/\alpha$ and $P \sim 1/2$ in this limit. This tells us that the spin bonds along the chains become much weaker than the bonds along the rungs which gain in strength.

Figure 5 displays Q and P versus α obtained using the numerical solution for Eqs. (39) and the approximate expressions in Eqs. (42) and (44). The agreement between the analytical and numerical results is noticeably good. As is evident in Fig. 5, for $\alpha > 2.5$, the large-α expressions agree well with the exact results. For $\alpha < 0.5$, the agreement between the small-α expressions and the exact results is also very good.

2. Zero-field and high-temperature regime

It is important that we discuss here the temperature dependence of the mean-field parameters Q and P. If Q and/or P vanished at a certain nonzero temperature, then a phase transition driven by thermal fluctuations would take place. However, this is not the case because both parameters do not vanish at any temperature. To prove this, we calculate Q and P in the high-temperature limit. Consider the limit $k_B T \gg J \gg J_\perp$ for simplicity. We expand the Fermi-Dirac factors to get $n_F[E_-] - n_F[E_+] \approx \frac{\epsilon}{2k_B T}$ to order 1 in $\beta E_\pm$, with $E_\pm = \pm\epsilon(k)$ if $h=0$. Substituting this into (39) leads to

$$Q \approx \frac{J}{8k_B T} \frac{1}{1 - \frac{J}{4k_B T}},$$

$$P \approx \frac{J_\perp}{8k_B T} \frac{1}{1 - \frac{J}{4k_B T}}, \tag{45}$$

which are valid in zero field. This shows that both Q and P decrease as temperature increases following a Curie-Wiess T^{-1} law, but they never vanish. The approximate expression for Q in (45), which is obtained in the limit $k_B T \gg J \gg J_\perp$, is the same as in 1D in the high-T regime and compares well with the exact numerical result depicted in Fig. 6(a), where $\alpha = 0$. Equations (45) clearly show that no phase transition driven by thermal fluctuations occurs in the ladder when the field is zero. Figures 6(b) and 6(c) display Q and P as functions of T/J for two nonzero values of the rung coupling. This again shows that there does not exist a temperature where Q and P vanish. The situation is different for the ground-state ($T=0$) field dependence. As in the case of the Heisenberg chain, we will show that a field-driven quantum phase transition occurs in the two-leg Heisenberg ladder exactly at the field corresponding to the onset of magnetization saturation.

C. Quantum phase transition in the two-leg ladder

First, we present the results for Q, P, and M_z as functions of the field h, which are obtained by solving numerically Eqs. (39). Then, we examine these equations analytically later on in zero T. In Figs. 7(a) and 7(b), Q, P, and M_z are drawn versus h/E_g for two values of the rung coupling α. In Fig. 7(a) temperature is $T = 0.025J$, whereas $T = 0.28J$ in Fig. 7(b). For the two-leg ladder, the critical field above which the higher-energy band $E_+(k)$ becomes completely occupied is obtained by stating that the maximum energy at $k = \pi/2$ becomes negative: $E_+(\pi/2) < 0$ which gives

$$h > h_{c2} = J\left(1 + \frac{\alpha}{2}\right) + J\sqrt{1 + \frac{\alpha^2}{4}}. \tag{46}$$

To derive Eq. (46), we set $Q = P = 0$ and $M_z = 0$ in $E_+(\pi/2)$. Figure 8 displays the higher-energy band $E_+(k)$ for $\alpha = 0.5$ and several magnetic fields. One notices that E_+ becomes completely negative for $h \approx 2.27J$. The latter is in agreement with the result $2.28J$ obtained from Eq. (46) when $\alpha = 0.5$.

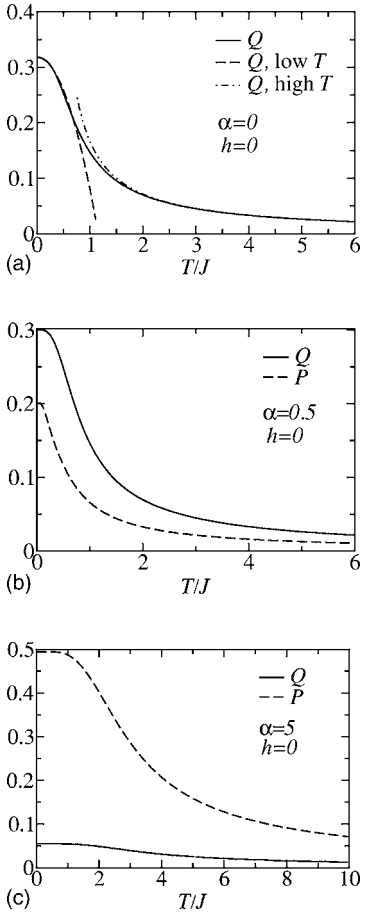

FIG. 6. The bond parameters Q and P are drawn vs temperature for $\alpha=0$ in (a), $\alpha=0.5$ in (b), and $\alpha=5$ in (c). Note that $P=0$ for $\alpha=0$. The magnetic field is zero in all three cases.

Also, for all those fields smaller than the energy gap—i.e., $h<h_{c1}=E_g$ at zero temperature—the energy band $E_+(k)$ remains above zero, causing the occupation level to remain at half-filling. Thus, according to the last of Eq. (39), the magnetization remains zero. Indeed, Figs. 7(a) and 7(b) show that the magnetization is zero at very low temperature for fields smaller than the energy gap. This is in good agreement with the results of Hayward, Poiblanc, and Lévy,[4] obtained using the exact diagonalization technique. Our curves for the magnetization versus field look very similar to theirs. At zero temperature, M_z increases from zero to saturation for fields $h_{c1}<h<h_{c2}$. Figure 7(a) displays this behavior for M_z at $T=0.025J$.

Another interesting phenomenon happens when we fix the magnetic field and vary the rung coupling in the regime where magnetization is nonzero. The magnetization decreases then vanishes at a critical value of α. Figure 9 illustrates this behavior for $T=0.027J$ and $h=0.5$. This figure shows also Q and P versus α, which continue to be nonzero even when M_z vanishes. Thus, the vanishing of M_z alone in this case is not enough to speak about a quantum phase transition in the same sense as before, because the order parameters Q and P do not vanish.

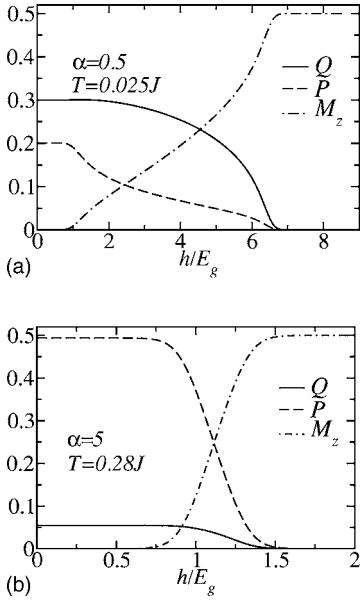

FIG. 7. The bond parameters Q and P and the magnetization are plotted as functions of h/E_g, where E_g is the energy gap in zero field and zero temperature. Note that the magnetization has two plateaus, one occurring at low fields ($h<h_{c1}$) and the second one at high fields ($h<h_{c2}$).

1. Calculation of Q and P near criticality when $\alpha \gg 1$

To show beyond doubt that a quantum phase transition occurs in the two-leg ladder as well, we consider the large and small-α limits and carry on the calculation analytically at zero temperature. In the limit $\alpha \gg 1$, $h_{c2} \approx J(1+\alpha+1/\alpha)$. For a field slightly smaller than the critical value h_{c2}, only a small portion of the higher-energy band $E_+(k)$ remains above the zero-energy axis. This will correspond to wave numbers satisfying

$$J_1^2 \sin^2 k > (h - J - J\alpha)(h - J) \tag{47}$$

if we let $M_z \approx 1/2$ for h only slightly smaller than h_{c2}. Let $\delta = h - h_{c2}$ with $0 < \delta \ll h_{c2}$. In this case $(h-J-J\alpha)(h-J) \approx J^2(1-\delta h_{c2}/J^2)$ for $\alpha \gg 1$. Also near h_{c2}, $Q \sim 0$, so that the condition (47) yields $k > k_0$, with $k_0 = \sin^{-1}(1-\delta h_{c2}/2J^2) \approx \pi/2 - \sqrt{\delta h_{c2}}/J$. Using this analysis in Eqs. (39), we get

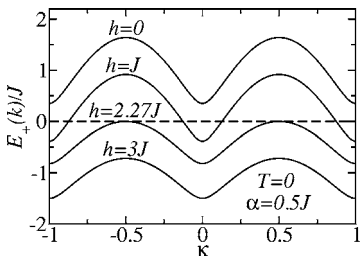

FIG. 8. The energy spectrum $E_+(k)$ is drawn versus $\kappa = k/\pi$ for several values of the field h. The dashed line represents the chemical potential for the JW fermions. Note that this higher-energy band sinks below the Fermi level when the field is greater than $h_{c2}=2.28$ for $\alpha=0.5$, Eq. (46).

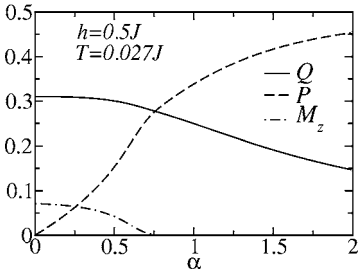

FIG. 9. Very interestingly, the perpendicular coupling α causes the magnetization to vanish. This is illustrated here for $h=0.5J$ and $T=0.027J$. This reflects the competition between the ferromagnetic ordering and the tendency to form spin singlets on the rungs.

$$Q \approx \frac{\sqrt{h_{c2}}}{J\alpha\pi}(h_{c2}-h)^{1/2},$$

$$P \approx \frac{\sqrt{h_{c2}}}{J\pi}(h_{c2}-h)^{1/2}, \tag{48}$$

for h slightly smaller than h_{c2}. For $h>h_{c2}$, $Q=P=0$ and $M_z=1/2$. These two equations clearly prove the occurrence of a zero-T phase transition at h_{c2} with the power exponent 1/2. This exponent is universal because it does not depend on α.

2. Calculation of Q and P near criticality when $\alpha \ll 1$

In this case $h_{c2} \approx J(2+\alpha/2+\alpha^2/8)$. Similarly, for $h \sim h_{c2}$, the integrals in Eqs. (39) yield

$$Q \approx \frac{\sqrt{2}}{\pi\sqrt{J}}(h_{c2}-h)^{1/2},$$

$$P \approx \frac{\alpha\sqrt{2}}{\pi\sqrt{J}}(h_{c2}-h)^{1/2}. \tag{49}$$

Note that when h_{c2} is replaced by $2J$ in the equation for Q in Eqs. (49), one recovers the same equation (22) as in the 1D case. Equations (49) also show that a zero-T phase transition occurs at h_{c2}. One can repeat the same analysis as in 1D for the bond-bond correlation function and find that a drastic change occurs at h_{c2}. Thus, a quantum phase transition takes place in the two-leg Heisenberg ladder as well at the α-dependent critical field h_{c2}.

D. Susceptibility versus magnetic field in the two-leg ladder

We now address the field dependence of the spin susceptibility. In Figs. 10(a) and 10(b), we display χ as a function of h for two values of α at several temperatures. We find that χ for the two-leg ladder behaves differently than the 1D susceptibility, essentially because of the energy gap. For $\alpha=0.5$ in Fig. 10(a), $\chi \sim 0$ for $h<E_g$ at low temperature ($T \ll E_g$). But as temperature increases, the influence of the gap decreases; for $T=0.3J$, χ looks very similar to the 1D susceptibility for the same temperature. Similarly, for $\alpha=1$ in Fig. 10(b), χ becomes nonzero when the effect of the gap is

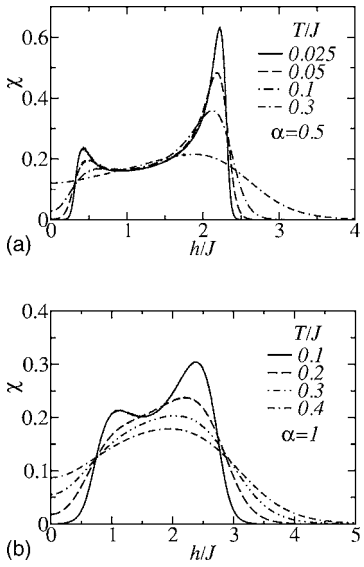

FIG. 10. The susceptibility of the two-leg ladder $\chi(h)=\partial M_z/\partial h$ is drawn versus h for $\alpha=0.5$ in (a) and $\alpha=1$ in (b).

overcome by the thermal excitations at enough high temperature. The peak at the upper critical field h_{c2} is shifted to a higher value for $\alpha=1$ because h_{c2} increases with α. At very low temperature, χ is characterized by two peaks, one near h_{c1} and the second one near h_{c2}. This is a consequence of the two plateaus that characterize the magnetization at low fields $h<h_{c1}$ and high fields $h>h_{c2}$. Note that the asymmetry in our two peaks is much more pronounced than in the results of Wang and Yu,[19] who used the transfer-matrix renormalization group. We think that this is a consequence of the approximations used in the present mean-field approximation. Also, our estimate of h_{c2} does not agree exactly with theirs.

VI. FIELD-TEMPERATURE PHASE DIAGRAMS

Figures 11(a) and 11(b) show the field-temperature phase diagrams for the Heisenberg chain and two-leg ladder with $\alpha=0.5$, respectively. The dashed lines are not critical lines but are crossover lines only. For the 1D case, the phase diagram is composed of three phases: the spin-liquid phase at zero field, the quantum ferromagnetic phase for field-temperature points to the left of the dashed crossover line,

$$T=0.2(h_c-h), \tag{50}$$

and the classical ferromagnetic state to the right of this line. The crossover line (50) ends with a QCP at the point ($T=0, h=h_{c2}$) shown as a solid dot. For the two-leg ladder, there are also three phases: the gapped-spin-liquid phase given at low fields and on the vertical axis T/J and the quantum and classical ferromagnetic phases, which are separated by a crossover line, that surprisingly has the same equation as (50) when the gap E_g is replaced by the value $0.35J$ it assumes for $J_\perp=0.5J$ and the field h_c by h_{c2}—i.e., $T=0.2(h_{c2}-h)$. These crossover lines are determined by locating for each temperature the field at which Q practically vanishes or M_z practically saturates. The lower-field cross-

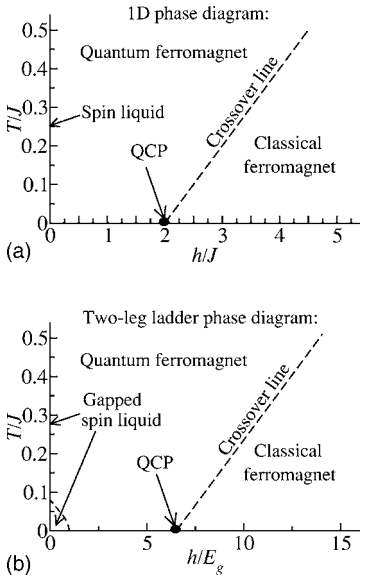

FIG. 11. The field-temperature phase diagrams we calculated in this work are displayed for the Heisenberg chain in (a) and the two-leg ladder with $\alpha=0.5$ in (b).

over line in Fig. 11(b) is determined by locating for each temperature the field where the magnetization becomes nonzero. The fact that this lower-field line curves towards the vertical axis is a result of the fact that growing thermal excitations wash out the gap and populate the higher-energy band with JW fermions that contribute to the magnetization. The vertical axis ($h=0$) represents the zero-field gapless phase (spin liquid) for the Heisenberg chain and the gapped spin liquid phase for the two-leg ladder.

The labeling of the ferromagnetic states as quantum or classical is consistent with the result of Parkinson and Bonner[3] for the Heisenberg chain who found that all the curves for magnetization divided by the spin S versus h/S saturate at the same value $h/S=4$ even for $S\to\infty$, where the quantum fluctuations become negligibly small; see Fig. 2 of Ref. 3. Differences between their curves, which correspond to different S values, occur in the quantum regime for fields smaller than h_c/S. The present finding of a finite-temperature crossover line ending with a QCP at zero temperature resembles the proposal for the existence of a QCP in high-temperature superconductors.[8] For the latter, chemical doping plays the role of the external parameter and the phase diagram is presented in terms of doping and temperature. There is evidence that the crossover line below which the pseudogap appears at finite temperature ends with a QCP near optimal doping at zero temperature.

In the high-T region (not shown) of the phase diagram, with $k_BT\gg J$ for the chain and $k_BT\gg\alpha J$ for the ladder, we find that

$$M_z\approx h/[4k_BT(1+J/2k_BT)],\quad k_BT\gg J \text{ or } k_BT\gg\alpha J, \tag{51}$$

which means that M_z does not vanish at a critical temperature and the upper regions of the phase diagrams in Fig. 11 are not limited by a critical line from above. One can rather speak of a crossover line from the low-T quantum ferromagnet regime to the Curie-like regime described by Eq. (51) in the high-temperature regime.

The phase diagram of the two-leg ladder looks like the experimental one proposed by Chaboussant *et al.*[7] for the two-leg ladder material $Cu_2(C_5H_{12}N_2)_2Cl_4$. However, it does not agree with the phase diagram calculated by Wang and Lu.[19] Physically, the saturation field should increase as temperature increases as a result of the need to compensate for the increasing thermal motion when the field attempts to align the spin moments. The crossover line starting at h_{c2} (the QCP) with a positive slope in our phase diagram reflects this fact, but the curve obtained by Wang and Lu does not; refer to Fig. 3 of Ref. 19.

VII. CONCLUSION

In this work, we study the magnetic-field-induced quantum criticality in the antiferromagnetic Heisenberg chain and two-leg ladder. We show that a quantum phase transition accompanying the saturation of the magnetization takes place in each of these two systems at the critical field h_c for the chain and at the upper critical field h_{c2} for the ladder. We also find that the phase transition in both systems is governed by the spin bond parameter, which vanishes at the critical value of the magnetic field where the zero-T magnetization saturates. The excellent agreement between our results and the existing exact numerically obtained results for the magnetization curves suggests that the present mean-field treatment is acceptable. The field-temperature phase diagrams are calculated for both systems. They are both characterized by a nonzero-temperature crossover line that ends with the quantum critical point (at zero temperature) at the field h_c for the chain and h_{c2} for the ladder. The way the bond order behaves as a function of temperature makes it a candidate for the so-called hidden order, which could be at the origin of the pseudogap behavior in high-T_C materials for example. We plan to persue further this proposal in the future.

ACKNOWLEDGMENTS

This work was supported by the Natural Science and Engineering Research Council of Canada (NSERC).

*Electronic address: mazzouz@laurentian.ca

[1] S. Sachdev, in *Quantum Phase Transitions* (Cambridge University Press, New York, 1999).
[2] J. C. Bonner and M. E. Fisher, Phys. Rev. **135**, A640 (1964).
[3] J. B. Parkinson and J. C. Bonner, Phys. Rev. B **32**, 4703 (1985).
[4] C. A. Hayward, D. Poilblanc, and L. P. Lévy, Phys. Rev. B **54**, R12649 (1996).
[5] R. Chitra and T. Giamarchi, Phys. Rev. B **55**, 5816 (1997).
[6] B. C. Watson, V. N. Kotov, M. W. Meisel, D. W. Hall, G. E. Granroth, W. T. Montfrooij, S. E. Nagler, D. A. Jensen, R. Backov, M. A. Petruska, G. E. Fanucci, and D. R. Talham, Phys. Rev. Lett. **86**, 5168 (2001).
[7] G. Chaboussant, Y. Fagot-Revurat, M.-H. Julien, M. E. Hanson, C. Berthier, M. Horvatić, L. P. Lévy, and O. Piovesana, Phys. Rev. Lett. **80**, 2713 (1998).
[8] J. L. Tallon and J. W. Loram, Physica C **349**, 53 (2001).
[9] M. Azzouz, Phys. Rev. B **48**, 6136 (1993).
[10] J. des Cloiseaux and J. J. Pearson, Phys. Rev. **128**, 2131 (1962).
[11] N. D. Mermin and H. Wagner, Phys. Rev. Lett. **17**, 1133 (1966).
[12] M. Azzouz, B. Dumoulin, and A. Benyoussef, Phys. Rev. B **55**, R11957 (1997).
[13] M. Azzouz and K. A. Asante, Phys. Rev. B **72**, 094433 (2005).
[14] M. Azzouz, L. Chen, and S. Moukouri, Phys. Rev. B **50**, 6233 (1994).
[15] E. Dagotto, J. Riera, and D. Scalapino, Phys. Rev. B **45**, 5744 (1992). Note that this paper addresses the effect of doping the two-leg Heisenberg ladder.
[16] T. Barnes, E. Dagotto, J. Riera, and E. S. Swanson, Phys. Rev. B **47**, 3196 (1993).
[17] T. Barnes and J. Riera, Phys. Rev. B **50**, 6817 (1994).
[18] Xi Dai and Zhao-bin Su, Phys. Rev. B **57**, 964 (1998).
[19] X. Wang and L. Yu, Phys. Rev. Lett. **84**, 5399 (2000).